Title: Past, Present, and Future: memory and choice encoding in prefrontal cortex of rats performing a double alternation task.

Abbreviated title: Working memory encoding in PFC during double alternation

Authors and author addresses:

Mathew Leonard[1,2,3] and Michael R. DeWeese[1,2,3]

1 Department of Physics, University of California, Berkeley, CA

2 Redwood Center for Theoretical Neuroscience, University of California, Berkeley, CA

3 Helen Wills Neuroscience Institute, University of California, Berkeley, CA

E-mail: deweese@berkeley.edu , leonard.mat@gmail.com

Corresponding Author:
Michael R. DeWeese, deweese@berkeley.edu

Number of Figures: 6 figures; no tables

Number of Pages: ??? (not including figures)

Keywords: auditory, cortex, prefrontal cortex, tetrode recording, extracellular, rat, neural coding, working memory, memory

Acknowledgements:

The authors are grateful for support from the McKnight Foundation, the Hellman Family Faculty Fund, and the National Science Foundation.

Past, Present, and Future: memory and choice encoding in prefrontal cortex of rats performing a double alternation task.

Abstract

Countless daily activities require working memory, but the cortical mechanisms underlying our ability to briefly store recent memories and use them to perform tasks are not well understood. We have trained rats to perform a delayed double alternation task in which rats alternate between entering one of two goal ports in a repeating left-left-right-right pattern. Performing above chance level requires subjects to store two separate pieces of information in memory. One strategy for performing the task is to recall the previous response and alternate between switching and repeating the previous response. For example, for the first "right" trial, the subject should recall that the previous goal was "left" and switch goals rather than repeat the previous goal as was done in the previous trial. Using tetrode recording in rats performing this task, we have found that some neurons in the prelimbic region of the medial prefrontal cortex (mPFC) encode the previous response during the delay period between behavioral trials. At the end of the delay period, when choosing a response goal, another group of neurons encode the switch or repeat decision. The chosen goal port is also encoded by yet another subset of neurons. Our results are consistent with the presumed role of rodent prelimbic mPFC in maintaining recently acquired task-relevent information and making decisions.

Introduction

Many studies in primates have found neural correlates of working memory in prefrontal cortex (PFC), such as sustained neural activity during periods when the subject must hold some information in memory. Many studies involve a delayed alternation (DA) task in which the subject alternates back and forth between two possible responses on subsequent trials separated by a delay (Jung et al., 1998; Baeg et al., 2003; Horst and Laubach, 2012). In primates, damage to PFC impairs performance on DA tasks (Gentile, 1972; Kojima et al., 1982) and stimulus-selective neurons exhibiting sustained activity during the delay period have been found in the dorsal-lateral region of PFC (Fuster and Alexander, 1971; Niki, 1974).

The role of PFC in rodent working memory is less well established. The granular dorsal-lateral PFC evident in primate cortex does not exist in rodents, but the medial PFC (mPFC) may be anatomically and functionally homologous (Uylings et al., 2003; Wise, 2008). Indeed, lesioning or temporarily inactivating mPFC in rodents is known to degrade DA task performance (Brito et al., 1982; Horst and Laubach, 2009). Accordingly, most working memory studies in rodents have targeted the prelimbic and infralimbic regions of medial PFC. In general, these studies have reported neurons that encode past goals during a delay period, but little evidence of sustained activity has been found (Baeg *et al.* 2003; Horst and Laubach 2012). However, the results of DA tasks are hard to interpret because

apparent encoding of goals might be explained by behavioral variability (Euston and McNaughton, 2006). Moreover, rats are known to use postural mnemonics for planned actions that could obviate the need for working memory (Chudasama and Muir, 1997). Finally, previous experiments involving standard DA have not been capable of discerning encoding of past actions from encoding of future actions, that is, "I came from here" compared to "I am going to there."

To address these issues, we have developed a self-directed delayed *double* alternation task. The rats were placed on a raised platform with three ports aligned horizontally on one wall. Rats performed the task by entering the center port and holding for 250-350 ms to initiate a trial, then choosing and moving to one of the side ports where they could receive a water reward. Correct responses resulting in rewards followed a left-left-right-right pattern. Since a past goal, "left" for example, can be followed by either "left" or "right" future goals, a rat's posture in the center port does not relay information about the correct reward port. With four possible trajectories, e.g. "left to right" (LR), trials can be grouped by past goal (LL, LR vs. RR, RL), by future goal (RL, LL vs. LR, RR), and by switch-stay trials (LR, RL vs. RR, LL), allowing us to separate memory from planning. Finally, approximately half of the trials were cued using a white noise burst from speakers positioned to the sides of the platform. The other trials were uncued, that is, identical sounds played from both speakers such that no information about the correct port was given to the rat. By doing this we intended to control for behavioral variability, because the rats made the same movements in two different contexts.

There are many possible strategies for performing this double alternation task, but at minimum, a subject need to retain two pieces of information. A possible strategy is to switch or repeat reward ports on subsequent trials. That is, an LL trial requires the rat to repeat the goal, the next trial, LR, requires the rat to switch goals. This strategy also requires rats to recall the past goal to correctly choose the future goal. Using the double alternation task, we assessed how neural activity in the prelimbic and infralimbic areas of mPFC encoded past goals, future goals, and switch-stay trials. We found that some neurons encoded the past goal in the delay period, when the rats move from the past reward port to the center port, and during the center hold period. Just before the rats left the center port, a small group of neurons became selective for switch-stay trials, suggesting that rats choose to switch or repeat reward ports and these neurons encode the choice. Shortly after rats chose to switch or stay, another group of neurons encoded the planned future goal. These results suggest the rats performed the double alternation task using the strategy described above, by recalling the previous goal and choosing to switch or repeat goals.

Methods

Subjects

Four male Long-Evans rats were trained on the delayed double alternation task. The rats had restricted access to water during training and testing, while food was available ad libitum. When performing the task, the rats were rewarded with water, which was supplemented afterwards in their home cages. All procedures were

approved by the Animal Care and Use Committee of the University of California, Berkeley (UC Berkeley).

Behavioral Task

We trained rats to perform a spatial delayed double alternation task. All training took place in a raised rectangular arena inside a soundproof box. The arena was open on three sides. The forth side contained three plastic ports arranged linearly. Each port contained an IR LED and a photodiode arranged on opposite sides. A computer system tracked the photodiode current to determine when the rats poked into the ports. The two side ports delivered 10 μl water drops from valves controlled via computer. Rats were water deprived for approximately 24 hours before training so the water drops were given as rewards.

The rats first learned to receive water rewards from the side ports by poking into each port. Then, the rats learned to initial trials by poking into the center port and getting rewards from the side ports. The rats were required to hold in the center ports for 250-350 ms, randomly chosen each trial. Once rats were able to perform more than 100 trials correctly, we began training them on a localization task. Two speakers were placed on the sides of the area, to the right and to the left of the ports. Bursts of white noise lasting 100 ms played from on speaker indicating the reward port, e.g. noise from the left speaker indicated a reward would be given from the left port. The rats were given 30 seconds to make a choice after initiating a trial, otherwise the trial was counted as a spoiled trial.

Once rats performed this localization task above 75% performance (75% correct responses), training on the double delayed alternation task began. The reward port changed in a set double alternating pattern, left-left-right-right-left-left-right-right and so on. When a rat made an error, the reward port stayed the same for the next trial. The task consisted of alternating blocks of cued and uncued trials, the L-L-R-R pattern continuing in each block. Cued trials were identical to the localization task. On uncued trials, white noise bursts played from both speakers such that the rat had no information about where to receive the reward. Blocks of cued trials lasted eight correct responses, while blocks of uncued trials lasted ten correct responses. Once a rat reached 75% performance on the DDA task, we performed an implantation surgery on the rat.

Surgical Procedure

For initial anesthesia, the subject was given an intraperitoneal injection of ketamine (90 mg/kg) and xylazine (10 mg/kg). Injections of muscimol (1.5 mg/kg) and Baytril (5 mg/kg) were given subcutaneously. The scalp was shaved and sterilized with iodine and ethanol. During the surgery, anesthesia was sustained with isoflurane (0.25%-0.75% of O_2 at 0.5 L/s flow). Under sterile conditions, the skull was exposed above the parietal, temporal, and frontal plates. Stainless steel screws were inserted cranium, two in the parietal plate, two in the right temporal plate, one in the left temporal plate, and one in the right half of the frontal plate. We performed a craniotomy centered 3 mm rostral from bregma above the left medial PFC. The craniotomy was rectangular, extending 2 mm in the rostral-caudal direction, and from the midline to 1.5 mm laterally. After removing the dura,

tetrodes were inserted into cortex 0.5 mm laterally from the midline at an angle of approximately 5° toward the midline to a depth of 1 mm from the surface of the cortex. The craniotomy was covered with agar. Afterwards, we covered the tetrode drive and skull screws with dental acrylic (methyl methacrylate). Post-surgery, the rat received a subcutaneous injection of buprenorphine (0.05 mg/kg) immediately, then 12 hours later. On the second and third day, the rat received a subcutaneous injection of muscimol (1.5 mg/ml).

Tetrodes and tetrode drives

We used tetrodes, four electrode wires twisted together, to record electrical signals from the cortex. Each wire in a tetrode was 12 μm in diameter and insulated with polyamide. One 50 cm long wire was drawn out, then cut in half. The halves were draped over a rod such that there were four equal length strands hanging down. A magnetic stirring rod was clipped to the end of the wires, then hung above a stirring plate. The rod was spun at approximately 60 rpm, for 3 minutes. Afterwards, a heat gun was used to melt the insulation together.

Movement of tetrodes after implantation was achieved using a custom-built tetrode drive. An HDMI connector was soldered to a custom designed PCB. Each pin of the HDMI connector is connected to a hole in the board. Individual wires of each tetrode are pinned into the holes with gold pins. A potentiometer was opened to expose the shuttle, then epoxied to the board. Polyamide tubes are glued to the shuttle then passed into larger polyamide tubes that are glued to the potentiometer casing. The four tetrodes are then passed through the smaller "support" tubes, then through the large "guide" tubes. All exposed wire was covered with scrap plastic and then dental acrylic.

The impedance of each wire was tested using a nanoZ (Tucker-Davis Technologies). To lower the impedance, we plated the electrodes with gold. Each tetrode was trimmed with a pair of serrated scissors. Then, the tips were immersed in 80 μL gold solution and 240 μL polyethelyene glycol (PEG) (Ferguson et al., 2009). Using the nanoZ, we passed 0.074 μA through each electrode until the impedance was lowered to approximately 300 kΩ.

Electrophysiological Recordings

Starting a week after the surgery, we recorded from rats while they performed the DDA task. A (Cyberlinks) neural signal processor recorded the voltage from all four tetrodes, sixteen signals in total, sampled at 30 kHz. Sorting the data occurred offline using custom code (available at https://github.com/mcleonard/spikesort). The raw data from each is filtered from 300 Hz to 6000 kHz to remove LFP and high frequency noise. The common average reference (CAR) is subtracted from each channel's data to remove artifacts and noise (Ludwig et al., 2009). Then, a voltage threshold is used to detect spikes in the processed data (Quiroga et al., 2004). For each threshold crossing, a 1 ms window is censored afterward to reject multiple detections. We then form tetrode waveforms by concatenating spike waveforms occurring simultaneously from the four electrodes in one tetrode.

The tetrode waveforms were then clustered using a Gaussian Mixture Model (GMM). First, we used Principle Components Analysis (PCA) to reduce the

dimensionality and identify features accounting for the most variance. Each waveform was reduced to the first ten PCA components. A GMM was then fit to the reduced waveforms. The best model was found by fitting models with varying numbers of clusters, from 5 to 30 then accepting the model with the smallest Bayesian Information Criterion (BIC). The clusters were visually inspected to identify putative neurons. The refractory period of neurons is reflected in the autocorrelation of spike times by a decrease in frequency at low (5-10 ms) inter-spike intervals (ISIs). Therefore, clusters without reduced counts at low ISIs are most likely occurring from noise or multiple neurons. A cluster with a clear dip in the autocorrelation is considered to contain spikes coming from a single neuron. Inspection of the cross-correlation of spike times between clusters allowed identifying clusters of spikes originating from the same putative neuron.

We synchronized the behavior and electrophysiology data using the stimulus onset for each trial. The voltage delivered to the speakers was recorded as an analog signal in the electrophysiology data. The behavior tracking system kept records of the stimulus onset as well. Using these time points, we synchronized the data and were able to calculate spike times relative to different behavioral events.

Histology

To identify the location of the tetrodes during the surgery, we performed histology using cresyl violet to stain the Nissl bodies in the brain matter. After recording was completed, we lesioned the area of the brain around the electrodes by applying a 3 μA current. The brain was extracted and fixed in 4% paraformaldehyde. Once the brains were well fixed, they were then transferred to a solution of 30% sucrose in 0.1 M PBS. Using a cryostat, the brains were sliced into 50 μm coronal sections. Each slice was then stained with cresyl violet to demonstrate Nissl substance in the neuron cell bodies. Lesions were then identified under a microscope.

Data Analysis

Data analysis was done using Python and various packages. All code and the IPython Notebook containing all the analysis in this paper are available at https://github.com/mcleonard/.

Peri-event histograms were calculated for analysis of neuron activity. The activity for each trial was represented by a binary spike train. For each trial, the spike train was convolved with a 30 ms wide normalized Gaussian kernel. The final peri-event histogram was found by averaging over trials.

Duration of memory retention

To calculate the maximum duration of memory retention, we calculated the performance, percent correct trials, for increasing delay durations. We then trained a Bayesian model on the performance data to calculate the delay duration where performance reached chance. The data, $\boldsymbol{y}$, was modeled with a normal distribution, with parameters μ and σ. A switch point, τ, was introduced which models the delay duration, t, where performance reaches chance (50%). The parameter μ was specified before the switch point τ as a linear function of α_1 and β_1, and after the

switch point as a linear function of α_2 and β_2. The priors were chosen to be as objective as possible as specified below:

$$\begin{aligned}
&\boldsymbol{y} \sim \text{Normal}(\mu, \sigma^2) \\
&\mu = \begin{cases} \alpha_1 * t + \beta_1 & if\ t < \tau \\ \alpha_2 * t + \beta_2 & if\ t \geq \tau \end{cases} \\
&\alpha_{1,2} \sim \text{Normal}(0, 0.01) \\
&\beta_{1,2} \sim \text{Uniform}(0, 100) \\
&\tau \sim \text{DiscreteUniform}(0, 20) \\
&\sigma \sim \text{Exp}(0.01)
\end{aligned}$$

The posterior, $P(\mu, \sigma^2|\boldsymbol{y})$, was sampled using the Metropolis-Hastings Markov Chain Monte Carlo (MCMC) algorithm. MCMC returned 70000 samples with a 20000 sample burn-in period, thinned by 5.

Population activity

To quantify the population activity, the activity (spike rate) of each neuron was first normalized by calculating the z-scores over time. Each trial was binned into 100 ms windows from 2 seconds before the stimulus onset to 2 seconds after the stimulus onset. The firing rate in each bin was taken as the number of spikes in the bin divided by the window width. Since the maximum firing rates of neurons varied widely, each neuron's average activity was normalized by calculating the z-score of each bin.

Due to the large variability in activity time courses, some neurons increasing in time, others decreasing in time, the neurons were clustered according to their average z-scores. Clustering was performed on PCA reduced waveforms with a GMM, varying the number of clusters and using the model with the smallest BIC. The average activity for each cluster was found by averaging the z-scores of the neurons in the individual clusters.

Variance explained by goals

Neuronal selectivity to past and future goals was determined using analysis of variances (ANOVA). The variance explained by goals was calculated using a two-way ANOVA to find the variance within groups, σ^2, and the variance between groups, σ^2_{PG}, σ^2_{FG}, and σ^2_{PG*FG}. The percent variance explained by a group

$$\frac{\sigma^2_X}{\sigma^2 + \sigma^2_{PG} + \sigma^2_{FG} + \sigma^2_{PG*FG}} \times 100,$$

where X is PG, FG, or $PG * FG$. The $PG * FG$ interaction gave the variance explained by switch-nonswitch trials, i.e. L-R and R-L vs. L-L and R-R trials. To ensure homoscedasticity i.e. equal variances within groups, we used the square roots of the firing rates as input for the ANOVA model.

Population selectivity

For population analyses, the activity of each neuron was taken in 50 ms bins from 1 second before to 1 second after time points in the trials (e.g. entering the center port, leaving the center port). In each time bin, a two-way ANOVA returned F-statistics and p-values for PG, FG, and the PG-FG interaction, for all neurons. The false discovery rate was constrained to 5% for each time bin (Benjamini and Hochberg, 1995).

For the analysis in Figures 6A-C, spike rates were found for each neuron from 50 ms before to 50 ms after the rat leaving the time points. The trials were split into two groups, left/right PG or left/right FG. The mean activity was found for each group by bootstrapping with 1000 samples. A significant difference in firing rates was tested using a two-tailed Mann-Whitney U test. The false discovery rate due to multiple comparisons was constrained to 5% using the Benjamini-Hochberg method (Benjamini and Hochberg, 1995).

In the analysis done in Figures 6D-F, the Stimulus Selectivity Index (SSI) was calculated to obtained a normalized value for stimulus preference. SSI was calculated from the bootstrapped mean activity found from the population analysis shown in Figures 6A-C:

$$SSI = \frac{r_{left} - r_{right}}{r_{left} + r_{right}}$$

Results

We recorded 223 neurons from 4 rats. Of those, only neurons with average firing rates above 0.5 Hz were selected. The remaining 197 neurons were further analyzed. Trials where the time from leaving the reward port to entering the center was greater than 20 seconds were discarded. Our analysis revealed nearly no differences between cued and uncued trials. Selectivity calculated with a one-way ANOVA, similar to the analysis used for goal encoding, showed only three significantly selective neurons over the entire task (Figure 5F). No other significant and/or consistent results were found. Therefore, all results reported below are analyzed with data from both tasks combined.

Behavior

We successfully trained rats to perform the double alternation task for both cued and uncued trials (see Figure 2B). The rats were trained for approximately two months from naiveté before reaching criteria performance (75% correct on uncued trials) for the full task. Performance worsened after surgery, but improved in the days after recovery while performing electrophysiological recordings, as shown in Figure 2A for one rat. Our behavioral task joins relatively few experiments using double alternation tasks with rats. One of the earliest successful double alternation tasks involved training rats to press a lever in a LLRR or UUDD pattern (Schlosberg and Katz, 1943). The authors presented each rat with a lever for 12 hours a day for four months. Out of 12 rats, 10 learned the task successfully. Two of the rats performing the UUDD task responded correctly on 59% and 67% of the first

50 trials averaged over three and half months of testing. Warburton and Heise (1972) reported a two-lever spatial double alternation task on which rats made zero errors in roughly 33% of LLRR blocks (averaged over 5 rats) (Warburton and Heise, 1972). Our three best-trained rats were able to complete 23%, 25%, and 45% (averaged over the final three recording sessions) of the 10 trial uncued blocks in a session with no errors. Warburton and Heise introduced a 10-second delay between trials, while we did not enforce any delay, which could explain the better performance on our task. However, it is possible that the rats used their posture in the delay period to indicate the next lever to push as seen in other experiments (Chudasama and Muir).

Task performance decreased as the time between leaving the reward port and initiating the next trial, the delay time, increased, as shown in Figure 2C. Regression analysis indicated the performance decreased significantly over time for both cued and uncued trials ($p < 1\times 10^{-5}$and $p < 1 \times 10^{-9}$, respectively). The time for performance to reach chance, the memory retention duration, was calculated using a Bayesian model. Posterior samples indicate the mean retention duration is 9.6 s (HPD 95% interval = {7.5 s, 12.5 s}) as shown in Figure 2D. Comparatively, rats performing a similar single alternation task with controlled delays perform at chance after a 20 second delay (Horst and Laubach, 2012). In an experiment involving monkeys, control subjects performing a spatial alternation task reached chance after a 40 second delay (Levin et al., 1988). Other spatial alternation experiments involving radial arm mazes have reported memory retention after multiple hours, but this retention is not related to working memory because it is disturbed when landmarks near the experiment chamber are moved (Dudchenko 2004). From our results, we suggest that the higher cognitive demand of our task, holding two bits of information in memory, reduces the memory retention duration. However, it is possible that including a controlled delay period might improve performance for longer delay durations.

Past goal, future goal, and switch-stay selectivity in individual neurons

We expect neurons encoding working memory to be selective for specific stimuli. During the two-second interval around the time of choice, we looked for selectivity for the past goal and future goal. Figure 4A shows the activity of a neuron recorded during performance of the task grouped into four task trajectories. The increased activity during the center hold period for left-to-right and left-to-left trajectories indicate selectivity for past goals. As shown in Figure 4B, the neuron is significantly selective for past goal (Mann-Whitney U test, $p < 2.5 \times 10^{-5}$) over the center hold time period. Another neuron (Figure 4C) has increased activity for left past goals before choice and increased activity for right future goals after choice. Again, the neuron is significantly selective (Mann-Whitney U test, $p < 2.5 \times 10^{-5}$) for future goal during the period between choice and reward (Figure 4D). Finally, some neurons showed selectivity for switch-stay trials, that is, trials where the future goal is opposite or the same as the past goal. An example neuron with significant switch-

stay selectivity is shown in Figures 4E and 4F. This neuron is significantly selective approximately 20 ms before choice to 350 ms after choice.

Calculating the percent variance explained by trial factors demonstrates the stimulus time course of encoding for individual neurons. For the example neuron shown in Figure 4C and 5A, the variance explained by past goals peaks when the rat enters the center port and at the time of choice. The variance explained by future goals then increases, peaking at approximately 250 ms. The variance explained by switch encoding for the example neuron in 5B begins increasing 100 ms before the rat leaves the center port reaching roughly 20% at the time of choice. Lastly, past goals and future goals explain nearly 80% of the variance in the firing rate of the neuron shown in Figure 5C.

Population encoding of past goal, future goal, switch-stay, and errors

We then assessed the past goal, future goal, and switch encoding across the population as shown in Figure 5E. The percentage of selective neurons for each factor was calculated with a two-way ANOVA in 50 ms time bins spanning 1 second before choice to 1 second after choice. In each bin, the critical p-value for rejecting the null hypothesis was chosen such that the false discovery rate was $q < 5\%$.

In the delay period between leaving the reward port and entering the center port, roughly 15% of the population was significantly selective for past goal in any bin. The population selectivity for past goal peaked when entering the center port with approximately 25% (48/197) of the neurons being significantly selective. Over the center hold period, this population selectivity dropped to ~6% (12/197) of the neurons 100 ms before choice, then increased to ~16% (26/197) of the neurons at the time of choice. The two-way ANOVA analysis also tested the interaction between past goals and future goals, equivalent to a statistical test for switch-stay trial selectivity. Switch trial encoding begins just before leaving the center port, peaking at 16% (24/197) of the neurons being selective for switch trials in the 50 ms after leaving the center port. In the period where the rats moved to the reward port, roughly 7% of the neurons were selective for switch trials in each bin. Selectivity for future goal across the population increased rapidly starting at 50 ms to 100 ms after choice. The population selectivity reached a maximum at 150 ms after choice, with 51/197 (26%) of the neurons selective for future goal. The selectivity peaked again [50/197 (25%)] roughly when the rats reached the reward port. We also found that neurons in mPFC encode past response outcomes (Figure 5F). Roughly 10% of the neurons we recorded encoded the outcome of the previous trial, starting after the reward would have been delivered. We didn't find this outcome encoding at later times, for instance, during the center hold period. In a previous study, prospective encoding of outcomes was seen, but we did not record any such neurons (Horst and Laubach, 2012).

Time course of task encoding

To analyze the time course of goal encoding, we averaged the explained variance of subsets of neurons (Figure 5D). We identified selective neurons by comparing the

firing rates in 100 ms wide windows around relevant time points in the task. When entering the center port, 65/197 neurons showed selectivity for past goals (Mann-Whitney U test, $q < 0.05$, $p < 0.017$), as well as 36/197 (Mann-Whitney U test, $q < 0.05$, $p < 0.009$) at the time of choice. The intersection of these two sets was taken as a subset of neurons [27/197 (14%)] selective for past goal during the center hold period. The variance explained by past goal was calculated for each neuron in this subset and then averaged together. The average variance explained increases from the baseline approximately 200 ms before entering the center port where the maximum is reached. The encoding is sustained during the center hold period and then decreases back to baseline shortly after response choice. A subset of neurons selective for switch trials [15/197 ($p < 0.003$)] was found at the time of choice (Figure 6A). Again, the average variance explained for this subset was calculated. The switch-stay encoding increases abruptly 100 ms before choice, then peaks at approximately 8% just after choice. Lastly, a subset of neurons selective for future goal [54/197 ($p < 0.014$)] was found when the rats entered the reward port. The average variance explained for this subset increases 100 ms after choice and is sustained while the rat is in the reward port.

Population and individual neurons flip past goal preference during delay

Unexpectedly, we found that many of the PG selective neurons we recorded flip past goal preference between leaving the past reward port and entering the center port. We first analyzed the PG selectivity for each neuron in the population at two time points, when the rats leave the PG port (PG-out) and when the rats enter the center port (center-in). We also analyzed the goal selectivity when the rats entered the reward port (FG-in). The firing rate of each neuron was measured in a 100 ms bin around these time points for each trial, grouped by either PG or FG (Figures 6A-C). At the PG-out time point, 32/197 neurons and 15/197 neurons were selective for right and left PG, respectively (Mann-Whitney U test, $q < 0.05$, $p < 0.012$). At the center-in time point, 19/197 neurons and 46/197 neurons were selective for right and left PG, respectively. Lastly, at the FG-in time point, 54/197 neurons and 33/197 neurons were selective for right and left FG, respectively. Then, for each neuron at each time point, we calculated the Stimulus Selectivity Index (SSI) (Figure 6D). Plotting the SSI histograms together reveals a preference towards right PG selectivity at PG-out and a preference towards left PG selectivity at center-in. For each time point, the mean SSI and standard error of the mean are shown in Figure 6E. The means of the PG-out and center-in SSI distributions are significantly different than 0 (*t*-test, $p < 0.05$ and $p < 0.001$, respectively). The PG-out and center-in distributions were significantly different (Mann-Whitney *U* test, $p < 0.0001$), as well as the FG-in and center-in dsitributions (Mann-Whitney *U* test, $p < 0.0003$). Finally, we selected those neurons that were selective for PG at PG-out and center-in, as well as for FG at FG-in (15/197 neurons). We then plotted the SSI for these neurons at each time point (Figure 6F). Only three of the 15 neurons retain goal preference across these three time points.

Discussion

We have found neurons encoding past goals, a switch-stay strategy, response choice, and prior outcomes in the medial PFC of rats performing a spatial delayed double alternation task, suggesting that this area is involved in integrating the past, present, and future into actions. The double alternation task allowed us to group trials into four different trajectories – LL, LR, RR, RL – revealing selectivity for past goals, switch or stay trials, and the response goal (Figure 3). Selectivity for past goals during the delay period has been seen previously in a few experiments that recorded from rat mPFC (Baeg et al., 2003; Horst and Laubach, 2012). In our experiment, it seems that PG encoding neurons activate when the rat enters the center port, and then sustain the information during the center hold period (Figure 5D). Similar patterns of activity have been found in the dorsal-lateral prefrontal cortex (dlPFC) of monkeys (Warden and Miller, 2010). It appears that the past goal information is not loaded into working memory until the rat enters the center port, rather than when leaving the past goal port.

At the end of the center hold period, just after the go stimulus plays, neurons encoding a switch-stay strategy activate (Figures 5D and 5E). A similar result has been seen in the dlPFC of monkeys performing a cued switch-stay task (Tsujimoto et al., 2011). It is ambiguous exactly what the switch-stay encoding neurons in our study represent. They could recall the switch-stay choice from the previous trial, or they could be storing the choice for the next trial, or they neurons could encode a decision based on some external cue. Regardless, the successful performance of this task requires utilizing at least two bits of information and our results suggest these two bits are to switch or stay and the past goal.

We found neurons that encoded the future goal on approach to the reward ports, after the switch-stay choice was made. Similarly, a study of rats performing a two-armed bandit task found that neurons in the PL/IL areas encoded goal choice upon approach (Sul et al., 2010). Our analysis shows no evidence of future goal planning before the go stimulus, unlike in the frontal orienting field (FOF), an area associated with rat prefrontal cortex (Erlich et al., 2011).

Roughly 10% of the neurons we recorded encode trial outcome. This is similar to previous results in rats (Sul et al., 2010; Horst and Laubach, 2012). Outcome encoding has also been seen in the anterior cingulate area of rat mPFC (Hyman et al., 2013). The PL/IL areas of mPFC in rats are known to have connections with the ventral tegmental area (VTA) and nucleus accumbens (ACC), both of which are associated with reward (Gabbott et al., 2005; Vertes, 2006).

Unexpectedly, we also found that goal preference of individual neurons and the population shifted over time from the past goal port to the center port. At the past goal, the population of neurons preferred the right goal. However, when entering the center port, the population had shifted into preferring the left goal. Then later, the population had shifted back to preferring the right goal. Of the neurons selective at each of these time points (47, 65, and 87, respectively), only 15 were selective at the past goal port and the center port, while 12 of those were selective at all three time points. Of those 12 neurons, 9 of them switched goal

preference along with the population. This suggests that there are two functional groups of neurons, one encoding past goals (at the center port) and one encoding future goals (at and approaching the reward ports), and that we found at least 9 neurons that belong to both of these functional groups. This same separation of spatial goal encoding has been seen in PFC of monkeys (Genovesio et al., 2006). The difference in goal preference between the groups was also seen in a later experiment by the same group (Tsujimoto et al., 2008).

Our task included a control block consisting of cued trials such that the rats might use reference memory instead of working memory. However, our analyses failed to find a consistent or significant effect of cueing on neuronal activity. A possible explanation for this result is that the rats performed the same strategy regardless of cues because neurons in rat mPFC are known to code differently when switching strategies (Rich and Shapiro, 2009). It is reasonable to assume that the rats might not have been aware if the next trial would be cued or not, so always employed the same strategy. Also, we often observed rats leaving the center port towards the correct goal port before the go sound had played. In an alternation task in a T-maze, Dudchenko manipulated extramaze cues during the delay period (Dudchenko, 2001). Similar to our results, while the rats performed worse, they still performed above chance even though the cues weren't available.

A flaw in our experiment is that we did not control for the angle of the rats' heads in the center port. Indeed, rats coming from the left port often fixed their hindquarters and rotated the front legs and head to the center port. In this way, the head was pointed to the right for left past goal trials and pointed to the left for right past goal trials. This could be improved in the future by constraining the posture using barriers around the center port as in Horst and Laubach's (2012) experiment. However, a study of neural activity of freely moving rats found no neurons with activity correlated with head direction (Poucet, 1997). Another concern is that selectivity might arise from selectivity for positions between left and right goal ports. Previous research has shown that neurons in the mPFC are not spatially selective unless a location has relevance to the task being performed (Poucet, 1997; Hok et al., 2005). Also, many of the neurons selective for PG showed activity changing in time while the rat was stationary in the center port (see Figures 4A and 5A for examples). Secondly, 25% of the neurons were selective when the rats entered the center port, decreasing to nearly 5% later in the center hold period. It appears that there are network dynamics involving PG encoding while the rat is stationary. The switch-stay encoding can't be explained by position, head angle, or movement since all are opposite between switch trials (LR, RL) and between stay trials (LL, RR). Furthermore, the switch-stay encoding occurs before the rats leave the center port.

In conclusion, our results show that neurons in the medial PFC of rats are involved in multiple aspects of a complex spatial alternation task, both individually and as a population. Unlike all previous spatial working memory tasks in rats, the double alternation task allows us to separate past goals from future goals in the neuronal signal. This ability allowed us to find neurons that encode past goals, switch-stay strategy, and future goals. Along with neurons encoding outcomes, we have found neurons coding for nearly all cognitive aspects of the behavioral task.

The separation of past goal and future goal encoding populations in rat mPFC, along with our other results, present many parallels between dorsal-lateral PFC of monkeys suggesting that the two structures are likely to be homologous across the species. Finally, our results along with anatomical findings reveal that "affective/motivational and spatial/contextual information converge at [mPFC] for goal-directed actions," as Vertes suggest (Vertes, 2006).

Figures

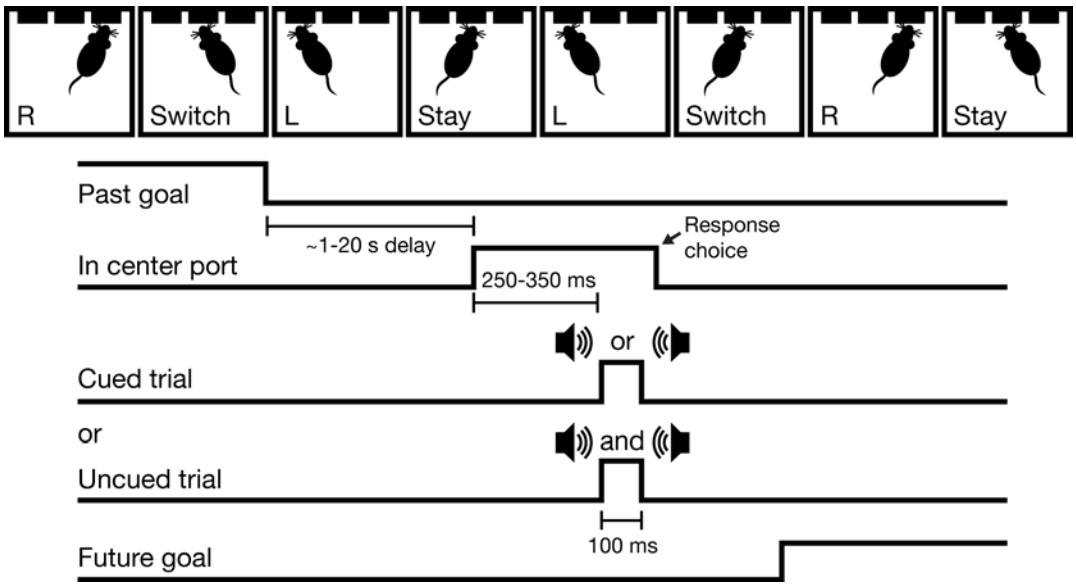

Figure 1. Task schematic, showing a cartoon of a rat performing the task and the task time course. Three ports are arranged linearly on one wall of a platform. Trials are initiated when the rat pokes its nose into the center port and holds there for

250-350 ms. Then, a 100 ms duration "go" sound plays, from either the left or the right speaker for cued trials, or from the left and right speakers for uncued trials. Responses are made to the side ports where a nose poke into the correct port results in a water reward. Correct goal ports follow a L-L-R-R pattern for both cued and uncued trials.

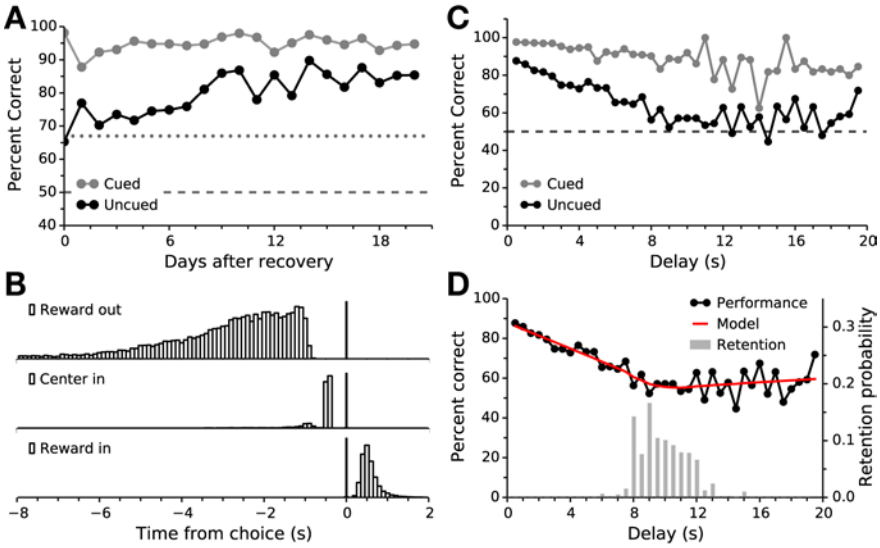

Figure 2. Behavior results. **A**, performance (percent of correct trials) over time for rat 3. Gray markers are performance on cued trials, black markers are performance on uncued trials. The dashed line denotes chance performance, and the dotted line denotes performance when using switch on error and single alternation strategies. **B**, normalized frequency of behavior events relative to the time of response choice. **C**, performance as a function of delay duration. The performance on both cued and uncued trials significantly decrease with increasing delay ($p < 1\times 10^{-5}$and $p < 1 \times 10^{-9}$, respectively) as measured by regression analysis. **D**, uncued trial performance as a function of delay duration with the trained Bayesian model's expected performance and retention duration posterior distribution samples (mean = 9.6 s, HPD 95% interval = {7 s, 12.5 s}).

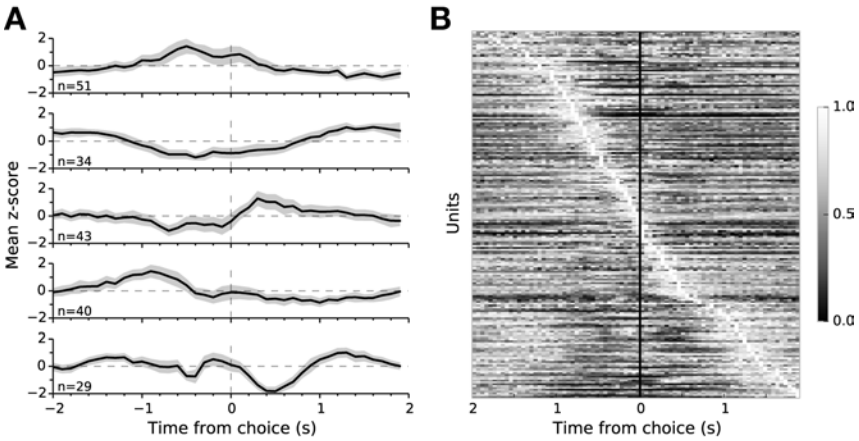

Figure 3. Population activity is modulated around choice time. **A**, the population of neurons clustered into five groups showing average z-scores and standard deviations in the group. **B**, normalized activity for each neuron, sorted by time of maximum activity.

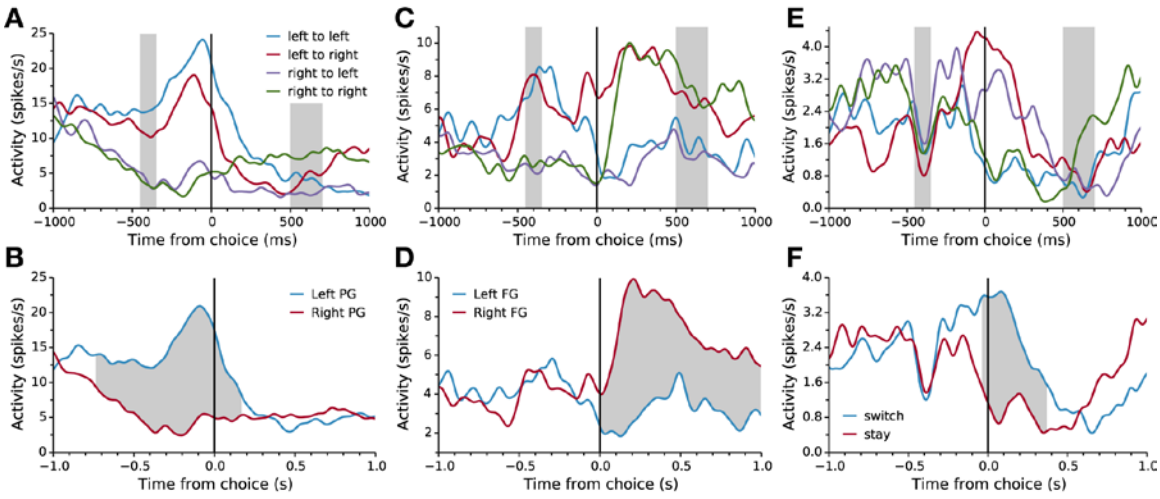

Figure 4, individual neurons encode past and future goals, and goal switching. **A**, **C**, **E**, peri-event histograms for individual neurons showing selectivity for past goal, future goal, and switch trials, respectively. Gray shaded areas indicate the time range for entering the center port (left area) and the time range for entering the reward port (right area). **B**, **D**, **F**, for the neurons shown in **A**, **C**, and **E**, the trials have been grouped together by past goal, future goal, switch-stay trials, respectively. Gray shaded area has significantly different firing rates (Mann-Whitney U test, $p < 2.5 \times 10^{-5}$).

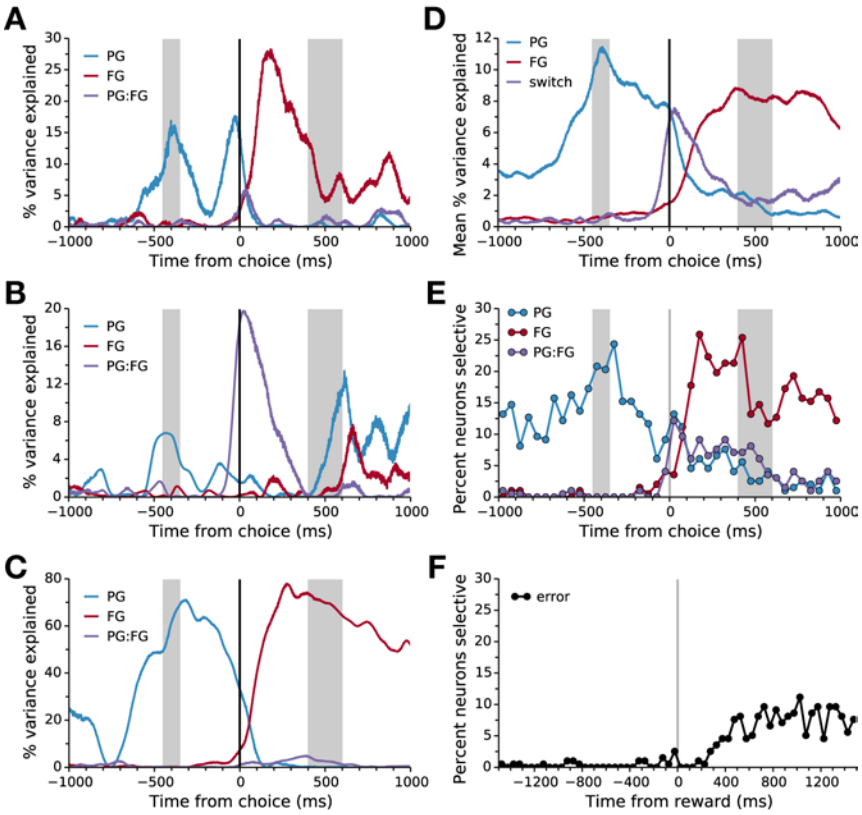

Figure 5. Selectivity analyzed by ANOVA. **A,** the same neuron as in **Figure 4C**, showing selectivity for PG when entering and leaving the center port, then selectivity for FG. **B**, a neuron showing selectivity for the PG-FG interaction indicating switch selectivity at the time of choice. **C,** a neuron showing strong selectivity for PG and FG. **D,** percent variance explained averaged over subsets of neurons selective for past goal, future goal, and switch trials. **E,** percent of neurons which are significantly selective over time in each of 50 ms bins for past goal (PG), future goal (FG), and switch trials. In each time bin, the false discovery rate was constrained to be less than 5%. **F**, same plot as **E**, but for percent of neurons selective for errors as tested by a one-way ANOVA.

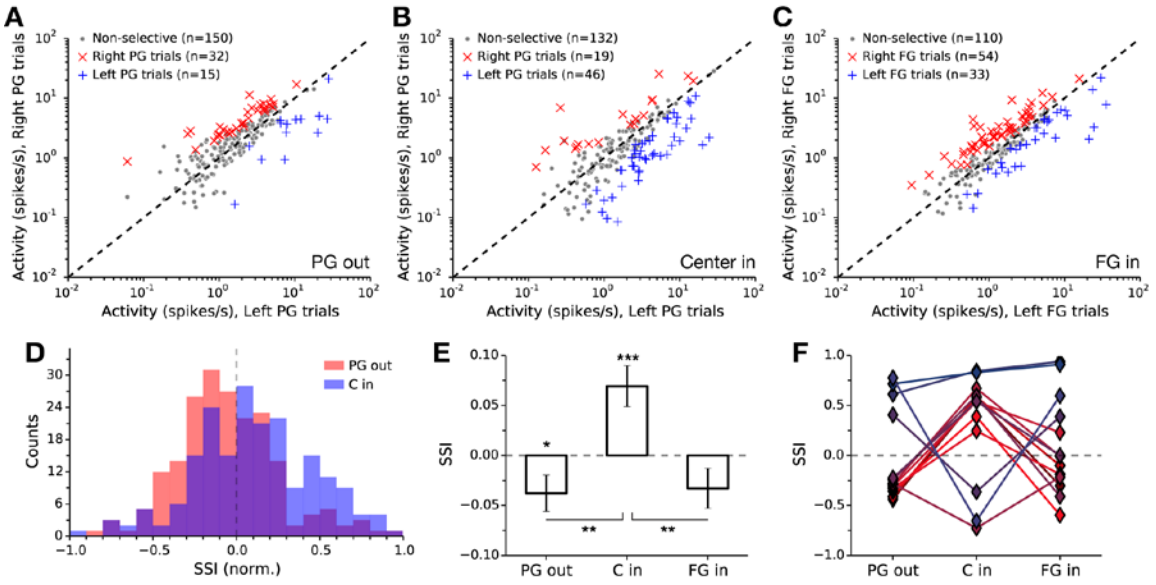

Figure 6, population and individual neuron goal preference changes across trial time points. **A**, Individual neurons show selectivity for past goal at the time of leaving the past goal port. Each point indicates the average activity of one neuron for left PG trials (x-axis) and right PG trials (y-axis) when leaving the past goal port. Neurons marked as × or + show a significant difference (Mann-Whitney U test, $q < 0.05$, $p < 0.02$) between left and right PG trials. **B**, same plot as **A**, but for spike rates found when entering the center port. **C**, same plot as **A** and **B**, but for FG selectivity when entering the FG port. **D**, histograms of Stimulus Selectivity Index (SSI) for PG calculated when leaving the PG port (red) and entering the center port (blue). **E**, bar plot showing the mean SSI for PG and standard error of the mean (SEM) of the population when leaving PG and entering the center port, and the mean SSI and SEM for FG when entering the FG port. Significance is designated as such, ∗: $p < 0.05$ (two-tailed *t*-test); ∗∗: $p < 0.0003$ (Mann-Whitney *U* test); ∗∗∗: $p<0.001$ (two-tailed *t*-test). **F**, SSI for neurons selective for PG when leaving the PG port, and entering the center port, and selective for FG entering the FG port. Each neuron is color-coded (red = right PG; blue = left PG) identically across time points, with the hue sorted by SSI at PG out.

References

Baeg EH, Kim YB, Huh K, Mook-Jung I, Kim HT, Jung MW (2003) Dynamics of Population Code for Working Memory in the Prefrontal Cortex. Neuron 40:177–188.

Benjamini Y, Hochberg Y (1995) Controlling the false discovery rate: a practical and powerful approach to multiple testing. J R Stat Soc Ser B … 57:289–300.

Brito G, Thomas G, Davis B, Gingold S (1982) Prelimbic Cortex, Mediodorsal Thalamus, Septum, and Delayed Alternation in Rats. Exp Brain … 46:52–58.

Chudasama Y, Muir JL (1997) A behavioural analysis of the delayed non-matching to position task: the effects of scopolamine, lesions of the fornix and of the prelimbic region on mediating behaviours by rats.

Dudchenko P a. (2001) How do animals actually solve the T maze? Behav Neurosci 115:850–860.

Erlich JC, Bialek M, Brody CD (2011) A cortical substrate for memory-guided orienting in the rat. Neuron 72:330–343.

Euston DR, McNaughton BL (2006) Apparent encoding of sequential context in rat medial prefrontal cortex is accounted for by behavioral variability. J Neurosci 26:13143–13155.

Ferguson JE, Boldt C, Redish AD (2009) Creating low-impedance tetrodes by electroplating with additives. Sens Actuators A Phys 156:388–393.

Fuster JM, Alexander GE (1971) Neuron activity related to short-term memory. Science (80-) 173:652–654.

Gabbott PL a, Warner T a, Jays PRL, Salway P, Busby SJ (2005) Prefrontal cortex in the rat: projections to subcortical autonomic, motor, and limbic centers. J Comp Neurol 492:145–177.

Genovesio A, Brasted PJ, Wise SP (2006) Representation of future and previous spatial goals by separate neural populations in prefrontal cortex. J Neurosci 26:7305–7316.

Gentile AM (1972) Movement organization and delayed alternation behavior of monkeys following selective ablation of frontal cortex. Acta Neurobiol Exp (Wars) 32:277–304.

Hok V, Save E, Lenck-Santini PP, Poucet B (2005) Coding for spatial goals in the prelimbic/infralimbic area of the rat frontal cortex. Proc Natl Acad Sci U S A 102:4602–4607.

Horst NK, Laubach M (2009) The role of rat dorsomedial prefrontal cortex in spatial working memory. Neuroscience 164:444–456.

Horst NK, Laubach M (2012) Working with memory: evidence for a role for the medial prefrontal cortex in performance monitoring during spatial delayed alternation. J Neurophysiol 108:3276–3288.

Hyman JM, Whitman J, Emberly E, Woodward TS, Seamans JK (2013) Action and outcome activity state patterns in the anterior cingulate cortex. Cereb Cortex 23:1257–1268.

Jung MW, Qin Y, McNaughton BL, Barnes C a (1998) Firing characteristics of deep layer neurons in prefrontal cortex in rats performing spatial working memory tasks. Cereb Cortex 8:437–450.

Kojima S, Kojima M, Goldman-Rakic P (1982) Operant Behavioral Analysis of Memory Loss in Monkeys with Prefrontal Lesions. Brain Res 248:51–59.

Levin E, Schantz S, Bowman R (1988) Delayed spatial alternation deficits resulting from perinatal PCB exposure in monkeys. Arch Toxicol 62:267–273.

Ludwig K a, Miriani RM, Langhals NB, Joseph MD, Anderson DJ, Kipke DR (2009) Using a common average reference to improve cortical neuron recordings from microelectrode arrays. J Neurophysiol 101:1679–1689.

Niki H (1974) Prefrontal unit activity during delayed alternation in the monkey. I. Relation to direction of response. Brain Res 68:185–196.

Poucet B (1997) Searching for spatial unit firing in the prelimbic area of the rat medial prefrontal cortex. Behav Brain Res 84:151–159.

Quiroga RQ, Nadasdy Z, Ben-Shaul Y (2004) Unsupervised spike detection and sorting with wavelets and superparamagnetic clustering. Neural Comput 16:1661–1687.

Rich EL, Shapiro M (2009) Rat prefrontal cortical neurons selectively code strategy switches. J Neurosci 29:7208–7219.

Schlosberg H, Katz A (1943) Double Alternation Lever-Pressing in the White Rat. Am J Psychol 56:274.

Sul JH, Kim H, Huh N, Lee D, Jung MW (2010) Distinct roles of rodent orbitofrontal and medial prefrontal cortex in decision making. Neuron 66:449–460.

Tsujimoto S, Genovesio A, Wise SP (2008) Transient neuronal correlations underlying goal selection and maintenance in prefrontal cortex. Cereb Cortex 18:2748–2761.

Tsujimoto S, Genovesio A, Wise SP (2011) Comparison of strategy signals in the dorsolateral and orbital prefrontal cortex. J Neurosci 31:4583–4592.

Uylings HBM, Groenewegen HJ, Kolb B (2003) Do rats have a prefrontal cortex? Behav Brain Res 146:3–17.

Vertes RP (2006) Interactions among the medial prefrontal cortex, hippocampus and midline thalamus in emotional and cognitive processing in the rat. Neuroscience 142:1–20.

Warburton DM, Heise GA (1972) Effects of scopolamine on spatial double alternation in rats. J Comp Physiol Psychol 81:523–532.

Warden MR, Miller EK (2010) Task-dependent changes in short-term memory in the prefrontal cortex. J Neurosci 30:15801–15810.

Wise SP (2008) Forward frontal fields: phylogeny and fundamental function. Trends Neurosci 31:599–608.